# Extension of the low diffusion particle method for near-continuum two-phase flow simulations

## Su Wei, He Xiaoying, Cai Guobiao *

*School of Astronautics, Beihang University, Beijing 100191, China*

**Abstract**   The low diffusion (LD) particle method, proposed by Burt and Boyd, is modified for the near-continuum two-phase flow simulations. The LD method has the advantages of easily coupling with the direct simulation Monte Carlo (DSMC) method for multi-scale flow simulations and dramatically reducing the numerical diffusion error and statistical scatter of the equilibrium particle methods. Liquid- or solid-phase particles are introduced in the LD method. Their velocity and temperature updating are respectively, calculated from the motion equation and the temperature equation according to the local gas properties. Coupling effects from condensed phase to gas phase are modeled as momentum and energy sources, which are respectively, equal to the negative values of the total momentum and energy increase in liquid or solid phase. The modified method is compared with theoretical results for unsteady flows, and good agreements are obtained to indicate the reliability of the one-way gas-to-particle coupling models. Hybrid LD–DSMC algorithm is implemented and performed for nozzle discharging gas–liquid flow to show the prospect of the LD–DSMC scheme for multi-scale two-phase flow simulations.

## 1. Introduction

In a number of aerospace engineering applications, gas flows involving a wide range of flow regimes are required to be simulated with accurate and efficient computational aerothermodynamics models. They can be characterized by the overall Knudsen number ($Kn$) and assorted with three different regimes.[1] The overall Knudsen number is calculated as

$$Kn = \frac{\lambda}{L} \tag{1}$$

where $\lambda$ is the mean free path and $L$ a characteristic length scale. The flow is treated to be continuum if the Knudsen number is smaller than 0.01. In this regime, intermolecular collisions dominate over other processes and equilibrate the inner structure of the gas. When the Knudsen number is much higher than 10, the flow regime is free-molecular and particle collisions with the surface play a critical role. Between the continuum regime and the free-molecular regime, there is the transitional regime, in which both the intermolecular collisions and the molecular–surface interactions are important.

Physical and computational aerothermodynamics models have been proposed for different flow regimes. In continuum regions, the gas velocity distributions are within small departure from equilibrium and the Navier–Stokes (N–S) or Euler equations are appropriate. Traditional computational fluid dynamics (CFD) schemes, which involve direct numerical

* Corresponding author. Tel.: +86 10 82316222.
  E-mail addresses: weisu@sa.buaa.edu.cn (W. Su), hexy@sa.buaa.edu.cn (X. He), cgb@buaa.edu.cn (G. Cai).

solutions for the governing equations, have been applied for the simulations of these flows. As the Knudsen number increases, the gas velocity distributions deviate a lot from equilibrium. The continuum assumption breaks down and models tied to kinetic theory are required to describe the gas flows. The Boltzmann equation, which is derived following the assumptions of molecular chaos and binary intermolecular collisions, is the governing equation for gas flows at arbitrary Knudsen numbers. However, the Boltzmann equation is a nonlinear integro-differential equation amenable to analytical solutions only for a small number of special problems, and numerical algorithms are required to solve this equation. The most widely used approach to solve the Boltzmann equation is the direct simulation Monte Carlo (DSMC) method, which has been developed since the early 1960s and has been successfully applied to a wide range of rarefied gas dynamics problems. The DSMC method abandons the form of the Boltzmann equation and computes gas flows through simulating the random evolution of a representative particle system.[2] Within a simulation time step, a collection of representative particles are tracked through a computation grid, which move and collide following the phenomenological models. The gas velocity distributions are represented by the velocities of those particles and the macroscopic properties of the flow are obtained by sampling the properties of the representative particles. Although the DSMC method is a mature approach for dilute gas simulations, the physical nature of the DSMC method, which requires high resolution of the mean free path and the collision rate by appropriate cell size and simulation time step, leads to higher computational expense at low Knudsen numbers when compared to traditional CFD schemes for the N–S equations, which often prohibits its application in near-continuum regimes.[3]

Efficient multi-scale computational models are needed to simulate multi-scale flows. Both traditional CFD and DSMC methods are usually applied. The CFD techniques are utilized in continuum regimes and the DSMC method is used where the continuum breaks down. Many researchers have focused on this type of computational model and proposed several simulation strategies. The simplest hybrid approach decouples the CFD and DSMC methods, which firstly performs the CFD simulation on a domain including a wide range of flow regimes and then defines inflow boundary for the independent DSMC simulation from the CFD results.[4,5] This uncoupled scheme is only used to simulate the steady state with the DSMC downstream of the CFD regions and the interface between the two regions is uniformly supersonic.[5] For more complex flow simulations, a coupled CFD–DSMC method is necessary. However, the large statistical scatter associated with the Monte Carlo method brings difficulties to information transfer across the interface, and scatter reductions also bring complexity and challenges to the numerical frameworks.

One of the efficient ways to overcome the difficulties of the hybrid CFD–DSMC scheme is to extend the DSMC method to near-continuum flow regimes. Among "all-particle" hybrid schemes, there are two main types of approaches. One is to modify the DSMC method to reduce its high computational expense in near-continuum regions, by either restricting the collisions of particles[6] or replacing them with resampling particle velocities from Maxwell distribution (equilibrium distribution).[7] The other is intermediated between the particle method and a conventional finite-volume solver for continuum flows, which represents the macroscopic flux by representative particles sampled from a certain shape of velocity distribution.[8] All these schemes are on the basis of local thermal equilibrium assumption (hence named equilibrium particle simulation method, EPSM) and provide results equivalent to a numerical solution of the compressible Euler equations. The utilization of same particles allows two-way strong information transfer in the hybrid scheme.[9] However, one of the main problems of these equilibrium particle methods is the large numerical diffusion errors. The probable reason is that the random molecular motions, which should be suppressed on the macroscopic level in near-continuum flows, are reproduced on the scales of computational cell sizes.[10]

An alternative approach to the equilibrium particle method for simulating near-continuum flows in the hybrid scheme has been proposed recently and named the low diffusion (LD) particle method.[9–15] In this DSMC similar method, a collection of representative particles are tracked through the grid in such a way that every particle maintains a constant relative position within a Lagrangian cell. The Lagrangian cell is a virtual cell that is coincident with the fixed computation grid at the beginning of each time step. During the time interval, the Lagrangian cells move and deform according to local flow properties. Particles follow the macroscopic motions of Lagrangian cells and random motions are suppressed. As a result, numerical diffusion error and statistical scatter associated with the existing continuum particle methods are greatly reduced. The LD method is firstly presented for the simulation of compressible inviscid gas flows and one-dimensional and two-dimensional test cases show it gives an equivalent solution to the Euler equations.[9] Then the LD method couples with the DSMC method to simulate multi-scale flows. The hybrid scheme is easily integrated in one numerical framework and easily implements two-way strong information transfer.[10] Many other modifications have been introduced to improve the LD method, including additions of viscosity effect,[11] rotational and vibrational nonequilibrium energy models,[12] determination of transport coefficients of gas mixtures,[13] and diffusive transport of nonequilibrium internal energy modes.[14] Subcell procedures, numerical weight and time step adaptations have also been applied to reduce cell size sensitivity and computational expense in the hybrid scheme. The LD–DSMC hybrid method has shown a promising prospect for simulations of high altitude rocket exhaust flows, flows around hypersonic reentry vehicles, and many other gas flows involving a wide range of characteristic length scales.[15]

In particular, two-phase flows consisting of liquid or solid particles in a carrier gas are commonly found in rocket exhaust plumes. These flows involve a wide range of flow regimes. Due to the combustion processes in the propulsion systems, the condensed phase particles are formed with very different sizes and properties. Unburnt drops of liquid propellants are one of the important classes of particles. Because of their small mass fractions, they might not affect the gas flow. However, they may cause significant contamination problems. There are several recorded accidents which were caused by plume contaminant. Additionally, in all types of aluminized propellants, aluminum oxide particles compose a large mass fraction of the exhaust and may significantly impact the gas flow properties. Soot must also be considered for liquid propellant thrusters, which are very important to the plume radiation characteristics.[16] Hence, numerical analysis should be carefully conducted for these flow simulations.

In this paper, an extension to the LD method is proposed to model the near-continuum two-phase flows. The momentum and energy exchanges between gas phase and dilute condensed-phase (liquid droplets or solid particles) are evaluated in each cell during each time step, which are used to modify the velocity and temperature values of both gas-phase and liquid- or solid-phase representative particles. The following sections are arranged as: in Section 2, the numerical methods, which include the basic LD method, extended LD algorithm, and the hybrid scheme, are described in details; in Section 3, a series of unsteady test cases are used to verify the modified LD method by comparisons with theoretical solutions; in Section 4, hybrid simulations are performed for a gas–liquid plume flow; finally, the paper concludes in Section 5.

## 2. Simulation methods

### 2.1. The basic LD method

The basic procedures of the LD method are described in details in the work of Burt and Boyd.[9] In the LD method, a large number of particles are tracked through the grid cells and represent the macroscopic motion of small fluid elements. As in the DSMC method, each particle carries the information of position, velocity used to update the position, and species identification. Each LD simulation particle is also assigned a temperature and a second velocity (as the bulk temperature and bulk velocity), which are used to represent the energy and momentum allocations of the fluid elements. The bulk temperature and velocity are updated during each simulated time interval according to the local flow properties. The representative particles move along with the Lagrangian cells. The Lagrangian cells are virtual cells and exactly represent the small fluid elements. The cell-average values are obtained by sampling the representative particles, and stored in the cell data structure.

The LD simulation procedures are modified from a DSMC calculation, and the following basic LD algorithm is performed during each time interval in place of DSMC collision calculations.[9]

(1) The cell-average values are calculated in each cell based on the particle's properties:

$$\boldsymbol{u}_{\text{cell}} = \langle \boldsymbol{u}_{\text{b},i} \rangle_{\text{m}} \tag{2}$$

$$T_{\text{cell}} = \langle T_{\text{b},i} \rangle + \frac{\langle m_i \rangle}{(3 + \langle \zeta_i \rangle)k} \cdot \frac{N_{\text{p}}}{N_{\text{p}} - 1} \\ \cdot (\langle \boldsymbol{u}_{\text{b},i} \cdot \boldsymbol{u}_{\text{b},i} \rangle_{\text{m}} - \langle \boldsymbol{u}_{\text{b},i} \rangle_{\text{m}} \cdot \langle \boldsymbol{u}_{\text{b},i} \rangle_{\text{m}}) \tag{3}$$

$$\beta = \sqrt{\frac{\langle m_i \rangle}{2kT_{\text{cell}}}} \tag{4}$$

$$\rho = \frac{\sum m_i W}{V_{\text{cell}}} \tag{5}$$

where the values $\boldsymbol{u}_{\text{cell}}$, $T_{\text{cell}}$, $\beta$, and $\rho$ are the cell properties of mass-averaged bulk velocity, temperature, thermal speed scale, and mass density, respectively; the values $\boldsymbol{u}_{\text{b},i}$, $T_{\text{b},i}$, $m_i$, and $\zeta_i$ are assigned to each particle, and are respectively, the particle bulk velocity, temperature, molecular mass, and the number of

internal degree of freedom (the subscript "$i$" is the index for particle identification); $k$ is the Boltzmann constant; $N_{\text{p}}$ the total number of particles within a cell; $W$ the number weight, i.e., the number of molecules represented by each simulated particle; and $V_{\text{cell}}$ the cell volume. The operators $<>$ and $<>_{\text{m}}$ denote respectively, an unweighted average and a mass-average of all particles in a cell.

(2) The outward normal velocity $u_{\text{f}}$ is evaluated for each Lagrangian face. At the start of each time step, the Lagrangian cell is coincident with the fixed grid cell, and the face is modeled as a massless and non-porous wall from which any colliding gas molecule will be specularly reflected. According to the kinetic theory, the Lagrangian face velocity is obtained from the following equations:

$$\frac{\rho_1}{\beta_1^2} \left[ s_1 \exp(-s_1^2) + \sqrt{\pi}(1 + \text{erf}(s_1))(\frac{1}{2} + s_1^2) \right] \\ - \frac{\rho_2}{\beta_2^2} \left[ s_2 \exp(-s_2^2) + \sqrt{\pi}(1 + \text{erf}(s_2))(\frac{1}{2} + s_2^2) \right] = 0 \tag{6}$$

$$s_1 = \beta_1(\boldsymbol{u}_{\text{cell},1} \cdot \boldsymbol{n} - u_{\text{f}}) \tag{7}$$

$$s_2 = -\beta_2(\boldsymbol{u}_{\text{cell},2} \cdot \boldsymbol{n} - u_{\text{f}}) \tag{8}$$

where $s_1$ and $s_2$ are speed ratios, Cell 1 and Cell 2 two cells separated by a face, and $\boldsymbol{n}$ is the outward normal unit vector respect to Cell 1. The face velocity $u_{\text{f}}$, which is solved using a certain iterative algorithm, guarantees the local thermal equilibrium and conservations of momentum and energy within a Lagrangian cell. And erf($\bullet$) is the error function.

(3) The bulk velocity and temperature of each particle are updated. The bulk velocity and temperature of particles are the same as those of the cell, which are updated by considering the momentum and energy transfer across the Lagrangian faces during a time step.

$$\boldsymbol{u}_{\text{b},i} = \boldsymbol{u}_{\text{cell}}^k = \boldsymbol{u}_{\text{cell}}^{k-1} + \frac{1}{\rho V_{\text{cell}}} \sum_{f=1}^{N_{\text{f}}} \Delta \boldsymbol{M}_f \tag{9}$$

$$T_{\text{b},i} = T_{\text{cell}}^k = T_{\text{cell}}^{k-1} \\ + \frac{2\langle m_i \rangle}{(3 + \zeta_i)k} \left[ \frac{1}{\rho V_{\text{cell}}} \sum_{f=1}^{N_{\text{f}}} \Delta E_f - \frac{1}{2} \left( \boldsymbol{u}_{\text{cell}}^k \cdot \boldsymbol{u}_{\text{cell}}^k - \boldsymbol{u}_{\text{cell}}^{k-1} \cdot \boldsymbol{u}_{\text{cell}}^{k-1} \right) \right] \tag{10}$$

$$\Delta \boldsymbol{M}_f = -2A_f \Delta t \varphi_f \boldsymbol{n}_f \tag{11}$$

$$\Delta E_f = -2A_f \Delta t u_f \varphi_f \tag{12}$$

$$\varphi_f = \frac{1}{2\sqrt{\pi}} \cdot \frac{\rho}{\beta^2} \left[ s_f \exp(-s_f^2) + \sqrt{\pi}(1 + \text{erf}(s_f))(\frac{1}{2} + s_f^2) \right] \tag{13}$$

where $\Delta \boldsymbol{M}_f$ and $\Delta E_f$ represent the total momentum and energy transfer into the corresponding cell across the Lagrangian face $f$ during a time interval $\Delta t$. While $A_f$, $\varphi_f$, $N_f$ and $\boldsymbol{n}_f$ are the face area, momentum flux, number of the Lagrangian faces and outward normal unit vector of the face. The superscript $k$ is the index of time step.

To take viscosity into account, the diffusive momentum and energy transport should be added. The diffusive transport contributions are determined through an explicit finite-volume solution to the viscous portion of the compressible N–S equations.[11] In a two-dimensional planar simulation:

$$\Delta \boldsymbol{M}_j = \Delta t \sum_{f=1}^{N_f} A_f \left( \frac{4}{3} \mu \frac{\partial u'}{\partial x'} \boldsymbol{n}_j + \mu \frac{\partial v'}{\partial x'} \boldsymbol{t}_j \right)_f \quad (14)$$

$$\Delta E = \Delta t \sum_{f=1}^{N_f} A_f \left( K \frac{\partial T}{\partial x'} + \frac{4}{3} \mu \frac{\partial u'}{\partial x'} \boldsymbol{n}_j \cdot \boldsymbol{u}_j + \mu \frac{\partial v'}{\partial x'} \boldsymbol{t}_j \cdot \boldsymbol{u}_j \right) \quad (15)$$

where $\mu$, $K$, $\boldsymbol{u}_j$ and $T$ are the dynamic viscosity, thermal conductivity, bulk velocity, and temperature calculated at the face, respectively. Values $\boldsymbol{n}_j$ and $\boldsymbol{t}_j$ designate face outward normal and face tangent unit vectors, while $u'$ and $v'$ are the bulk velocity components normal and tangent to the face. The operator $\partial/\partial x'$ gives a derivative in the face outward normal direction. For a viscous flow simulation Eqs. (14) and (15) should be added to the right sides of Eqs. (11) and (12) to update the bulk properties.

(4) New position of Lagrangian cells after a time interval is evaluated according to the cell face velocity.
(5) Velocities used in the DSMC movement procedures to update the particle's position are calculated in a way that all particles maintain a constant relative position in a Lagrangian cell over the time step.

More details about the algorithm can be found in the Refs. [9–15]. The LD method is proposed on the deep comprehension about the physical phenomena. It can be figured out that the particles in the LD method represent the allocations of mass, momentum, and energy within fluid bulk. The macroscopic motions of the fluid bulk are described through the motion and deformation of the Lagrangian cells. The mass, momentum, and energy evolve according to both the kinetic theory and fluid equations, and transfer among grid cells by the motion of particles.

## 2.2. Modifications for near-continuum two-phase flows

In the proposed extension of the LD method to near-continuum two-phase flows, representative particles denoting the condensed phase (real solid particles in gas–solid flows, and liquid droplets in gas–liquid flows) are introduced and stored in a structure independent of the gas particles. The condensed-phase particle is modeled as an inflexible sphere and has self inner structure. Therefore, the particle can be treated as mass point and has its own diameter $d_j$, phase density $\rho_{p,j}$, velocity $\boldsymbol{u}_{p,j}$, temperature $T_{p,j}$, specific heat at constant pressure $C_{pp,j}$,

and position $X_{p,j}$. During each time step, liquid- or solid-phase particle moves at its own velocity, while the velocity and temperature are updated according to the gas aerodynamic drag and heat transfer between two phases, respectively.

To evaluate the relaxation processes of the two phases, several assumptions are introduced:

(1) The condense-phase particles are modeled as inflexible spheres with uniform temperature, which are not rotary.
(2) The inner relaxation time of gas phase is much shorter than that between two phases. Therefore, the local equilibrium holds in gas phase.
(3) The size of the condense-phase particle is small compared to characteristic gradient length scales in the gas. The flow around a particle is assumed as a uniform free stream.
(4) The blocking effect and the interactions among the condensed-phase particles are negligible. This assumption is enforced when the condensed phase is dilute enough, which is common in aerospace engineering applications.
(5) There are no mass transfers between two phases, if no phase transition is considered.

### 2.2.1. Aerodynamic drag and particle motion

The aerodynamic drag acting on a single particle is given as[17]

$$\boldsymbol{F}_d = \frac{1}{8} \pi C_d d_j^2 \rho_{\text{cell}} |\boldsymbol{u}_{\text{cell}} - \boldsymbol{u}_{p,j}| (\boldsymbol{u}_{\text{cell}} - \boldsymbol{u}_{p,j}) \quad (16)$$

where $\rho_{\text{cell}}$ and $\boldsymbol{u}_{\text{cell}}$ are the mass density and bulk velocity of the cell in which the condensed-phase particles are located, and $C_d$ is the coefficient of drag.

The coefficient of drag used in the expression of the drag force may be defined as a constant or as a function of the fluid's Reynolds number $Re$. The coefficient of drag and Reynolds number are calculated as following[17]:

$$C_d(Re) = \begin{cases} \dfrac{24}{Re} & Re < 1 \\ \dfrac{24}{Re}\left(1 + \dfrac{1}{6} Re^{2/3}\right) & Re < 600 \\ 0.424 & Re \geqslant 600 \end{cases} \quad (17)$$

$$Re = \frac{\rho_{\text{cell}} d_{p,j} |\boldsymbol{u}_{\text{cell}} - \boldsymbol{u}_{p,j}|}{\mu} \quad (18)$$

$$C_d(Re) = \begin{cases} \dfrac{24}{Re}\left(1 + 0.15 Re^{0.687}\right)\left[1 + \exp\left(-\dfrac{0.427}{Ma^{4.63}} - \dfrac{3.0}{Re^{0.88}}\right)\right]\left\{1 + \dfrac{Ma}{Re}\left[3.82 + 1.28 \exp\left(-0.125 \dfrac{Re}{Ma}\right)\right]\right\} & Re \leqslant 1000 \\ 0.424\left[1 + \exp\left(-\dfrac{0.427}{Ma^{4.63}} - \dfrac{3.0}{Re^{0.88}}\right)\right]\left\{1 + \dfrac{Ma}{Re}\left[3.82 + 1.28 \exp\left(-0.125 \dfrac{Re}{Ma}\right)\right]\right\} & Re > 1000 \end{cases} \quad (19)$$

where $\mu$ is the dynamic viscosity of the local gas flow. If the particles are not sufficiently large in comparison to the local gas mean free path, the Carlson–Hogland formula should be used to consider the rarefaction effects[17]:

To consider the drag and gravity of a single particle, the motion equation of the particle is given as

$$\frac{\mathrm{d}\boldsymbol{u}_{p,j}}{\mathrm{d}t} = \boldsymbol{g} + \frac{\boldsymbol{F}_d}{m_{p,j}} \quad (20)$$

where $\boldsymbol{g}$ is the gravitational acceleration, and $m_{p,j}$ the mass of a single particle.

### 2.2.2. Heat transfer and temperature relaxation

Heat transfer occurs when temperature difference exists between two phases. The quantity of heat is in proportion to both the temperature difference $T_{\text{cell}} - T_{\text{p},j}$ and the surface area of heat transfer, which is calculated as[17]

$$Q_{\text{p},j} = (Nu)\pi d_{\text{p},j}K(T_{\text{cell}} - T_{\text{p},j}) \tag{21}$$

where $Nu$ is the Nusselt number, which is used to describe the contribution of gas motion to the heat transfer. The Nusselt number is given as

$$Nu = 2 + 0.6Pr^{1/3}Re^{1/2} \tag{22}$$

where $Pr$ is the Prandtl number, and is defined as

$$Pr = \mu C_{p\text{cell}}/K \tag{23}$$

Prandtl number describes the physical property of the gas phase. The value $C_{p\text{cell}}$ is the local special heat of the gas at constant pressure. When the Knudsen number based on the ratio of the mean free path to the condensed particle size is larger than 0.1, the flow is considered dilute for particles. The rarefaction effect will weaken the heat transfer and a correction should be added to the calculation of the Nusselt number. In a common situation, the Nusselt number is corrected as[18]

$$Nu = Nu_0 \frac{1}{1 + 2.72\frac{Kn_0}{\sqrt{\gamma_g}Pr}Nu_0} \tag{24}$$

where $Kn_0$ is the Knudsen number calculated by using the condensed particle size as the characteristic length, $\gamma_g$ the specific heat ratio of gas flow, and $Nu_0$ the Nusselt number calculated from Eq. (22).

The temperature change may be expressed as[17]

$$m_{\text{p},j}C_{pp,j}\frac{\mathrm{d}T_{\text{p},j}}{\mathrm{d}t} = Q_{\text{p},j} + m_{\text{p},j}q_{\text{p}} \tag{25}$$

where $q_{\text{p}}$ is external heat ratio, and $C_{pp,j}$ is the condensed-phase special heat at constant pressure. In most of cases, $C_{pp,j}$ is treated as a constant. For liquid phase, it may be expressed as a function of temperature.[19]

### 2.2.3. Particle-to-gas effect model

The back influence transferred into the gas phase, due to acceleration and heat of condensed phases, is modeled as momentum and energy sources, which are respectively, equal to the negative values of the total momentum and energy increase in condensed phase. It satisfies a conservation of the system momentum and energy. The momentum and energy that the gas fluid bulk obtains during a time interval can be easily calculated as

$$\Delta \boldsymbol{M} = -\sum_{j}^{N_{\text{p,p}}} m_{\text{p},j}\Delta \boldsymbol{u}_{\text{p},j} \tag{26}$$

$$\Delta E = -\sum_{j}^{N_{\text{p,p}}} \left( Q_{\text{p},j} + \frac{1}{2}m_{\text{p},j}\Delta|\boldsymbol{u}_{\text{p},j}|^2 \right) \tag{27}$$

where $N_{\text{p,p}}$ is the total number of condensed-phase particles within fluid bulk.

### 2.2.4. Numerical procedures

In the numerical procedures, an additional loop for all the condensed-phase particles is performed to update the velocity and temperature during a time interval based on the local properties of gas flow. The motion of these particles should also be added into the particle movement routine. During a time interval $\Delta t$, the velocity $\boldsymbol{u}_{\text{p},j}$, temperature $T_{\text{p},j}^k$, and position $\boldsymbol{X}_{\text{p},j}^k$ of the particle are evaluated as

$$\boldsymbol{u}_{\text{p},j}^k = \boldsymbol{u}_{\text{p},j}^{k-1} + \Delta t\left( \boldsymbol{g} + \frac{\boldsymbol{F}_d}{m_{\text{p},j}} \right) \tag{28}$$

$$T_{\text{p},j}^k = T_{\text{p},j}^{k-1} + \frac{\Delta t}{m_{\text{p},j}C_{pp,j}}(Q_{\text{p},j} + m_{\text{p},j}\tilde{q}_{\text{p}}) \tag{29}$$

$$\boldsymbol{X}_{\text{p},j}^k = \boldsymbol{X}_{\text{p},j}^{k-1} + \Delta t \cdot \boldsymbol{u}_{\text{p},j}^k \tag{30}$$

where $\tilde{q}_{\text{p}}$ is exterior heat source.

For the LD simulation of gas, all simulations are performed as listed above, but cell-based bulk velocity and temperature values should be updated to consider momentum and energy transfer from condensed phase. In other words, to update the bulk velocity and temperature in Step (3) in Section 2.1, the values of Eqs. (26) and (27) should be added to Eqs. (9) and (10), respectively.

### 2.3. Hybrid LD–DSMC algorithm

The LD method has been integrated in a DSMC code for the simulation of flows involving both continuum and nonequilibrium regions.[10] In the hybrid algorithm, the LD simulation is performed in continuum regimes, while DSMC calculation is used in nonequilibrium regions. A continuum breakdown parameter is periodically evaluated and is compared with a threshold value to determine whether each grid cell should be assigned to either DSMC or LD domains.[11] Two layers of buffer cells are employed along the boundary between DSMC and LD domains. During each computation time step and before the motion routine, new representative particles of either DSMC or LD types are created in the two layers based on the local flow properties. In the motion routine, these created particles carry local flow information and move across the interface of continuum and nonequilibrium regions. This scheme easily couples two-way strong information. After the movement, some of the information-transfer particles are discarded.

The implementation of the LD method for two-phase flows in a hybrid LD–DSMC code is the same as the proposed hybrid scheme. The basic DSMC code for two-phase flow simulations is developed by authors' group.[20] It is a parallel 2D-axial/3D simulation code, including Gallis' one-way gas–particle interaction model,[21] Burt's two-way coupled model,[22] and Gimelshein's gas–particle collision model.[16] A potential shortcoming may happen, when the condensed-particle-based Knudsen number is sufficiently high and Eqs. (19) and (24) are used to include the rarefaction effects in interphase moment and energy exchange. In this situation, as the particles cross the LD/DSMC boundaries, sudden changes in particle force or heat transfer rate may appear. One proper solution is to use the Green's function approach of Gallis, et al.[21] in LD domain to evaluate the condensed-phase relaxation, which

is of consistency with the approach currently used within the DSMC domain.

In hybrid algorithm, a continuum breakdown parameter is periodically calculated to determine the interface of continuum and nonequilibrium regions. Several continuum breakdown parameters have been proposed.[23–25] In the two-phase hybrid LD–DSMC simulation, the continuum breakdown parameter is given as[26]

$$Kn_{\max} = \max(Kn_D, Kn_T, Kn_V) \qquad (31)$$

and the Knudsen number is expressed as

$$Kn_Q = \frac{\lambda}{Q}|\nabla Q| \qquad (32)$$

where $Q$ is any flow property, and the flow density, temperature, and magnitude of velocity are considered here to account for the transport phenomena of viscosity and heat transfer. The threshold value of 0.05 is set, which can best predict the regions where continuum breaks down.[25]

## 3. Verification of two-phase flow modification

In this section, two simple cases are performed to independently test the motion and temperature relaxations for the condensed phases in LD simulations.

### 3.1. Particle motion with drag and gravity

A test is performed in order to check the implementation of the particle's basic equations of motion with both aerodynamic drag and gravitational forces.[27] It is assumed that a particle experiences forces due to presence of the fluid, but the fluid is not affected by the particle. The one-way interaction is used, and the behavior of the particles could be examined more closely without the intricacies involved in mutual fluid–particle interaction. A single particle is introduced in a two-dimensional domain and moves perpendicular to the direction, as illustrated in Fig. 1. The computation domain is set to be 0.02 m × 0.02 m, and the cells are divided on a scale of 0.005 m. The boundary condition is pressure outlet condition. The liquid phase is chosen as $C_{14}H_{30}$ and the gas phase is air. The initial conditions of the two phases are listed in Table 1. As the same as the reference work,[26] a constant coefficient of drag ($C_d = 1.2$) is used and the gravity is given a value of $g = 0.098$ m/s². Hence, the initial drag-to-gravitational force ratio is about 0.0148. Comparisons of liquid particle position, $x$-direction velocity, and $y$-direction
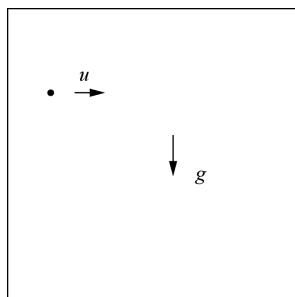
**Table 1** Initial conditions of test for drag and gravity.

| Phase | Species | Density (kg · m$^{-3}$) | Temperature (K) | Speed (m · s$^{-1}$) | Diameter (m) |
|---|---|---|---|---|---|
| Gas | Air | 1.16 | 300 | 0 | – |
| Liquid | $C_{14}H_{30}$ | 720 | 300 | 0.01 | $1.0 \times 10^{-4}$ |

velocity between simulation results and theoretical solutions are shown in Figs. 2–4. The results indicate that the equations of particle motion due to drag and gravity work very well.

### 3.2. Particle heating

This case is used to test the temperature relaxation of the condensed phase. A single liquid particle with relative higher velocity and temperature decelerates and cools down in still air. The one-way coupling is enforced, and the particle only
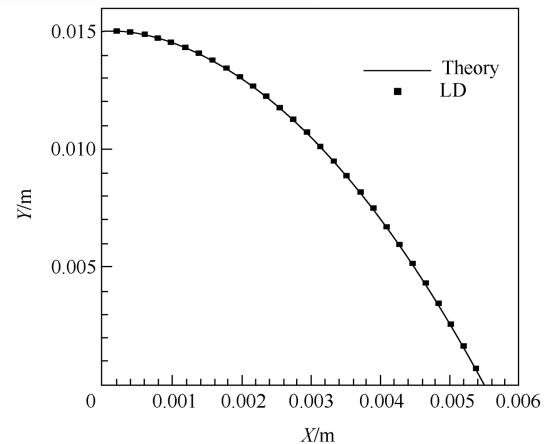


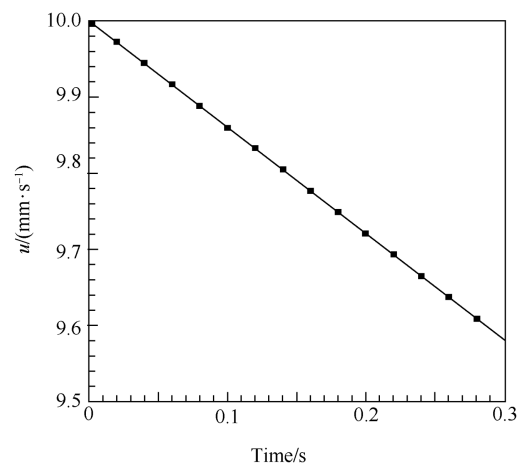**Fig. 2** Liquid particle position of test for drag and gravity.



**Fig. 3** Liquid particle $x$-direction velocity of test for drag and gravity.



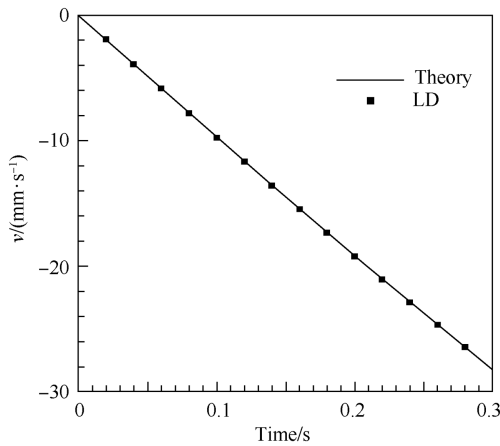**Fig. 1** Illustration of test for drag and gravity.

**Fig. 4** Liquid particle *y*-direction velocity of test for drag and gravity.

suffers an aerodynamic drag with a constant coefficient of drag set to be $C_d = 1.2$. The computation domain is used the same as the former test. The initial conditions of the two phases are listed in Table 2. Fig. 5 shows the temperature solutions from LD simulation and the theoretical solution. It is noted that the obtained LD solution is in good agreement with the theoretical solution.

**Table 2** Initial conditions of test for temperature relaxation.

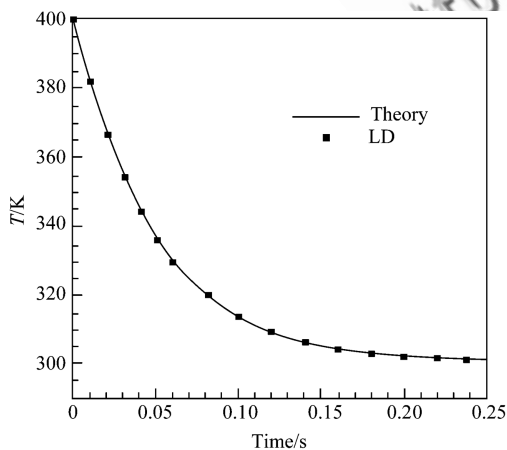| Phase | Species (m) | Density (kg·m$^{-3}$) | Temperature (K) | Speed (m·s$^{-1}$) | Diameter (m) |
|---|---|---|---|---|---|
| Gas | Air | 1.16 | 300 | 0.0 | – |
| Liquid | $C_{14}H_{30}$ | 720 | 400 | 0.01 | $1.0 \times 10^{-4}$ |



**Fig. 5** Liquid particle temperature of test for temperature relaxation.

## 4. Hybrid simulation for two-phase flows

Two-phase flows are commonly found in aerospace engineering applications. An application of interest for the present work is a thruster for satellite attitude control, which works in impulsive mode discharging gas–liquid flow and may result in contamination on the surface of sensitive components. The plume flow field should be calculated carefully to analyze the plume effects. The plume flow is complicated and contains both continuum and nonequilibrium regimes. The 2D-axial hybrid LD–DSMC code is performed for such a gas–liquid plume flow discharged from a nozzle into vacuum environment.

The thruster uses monomethylhydrazine (MMH, $CH_6N_2$) and nitrogen tetroxide (NTO, $N_2O_4$) as propellants. In order to obtain the inlet conditions of the gas flow and liquid droplets, an antecedent calculation is conducted at first. A quasi-1D model is used to simulate the gas parameters and droplet distribution in the thrust chamber,[28] while the gas flow and the droplets motions in the nozzle are simulated by coupling the solutions of the N–S equations and the droplets motion equations. The simulation results indicate that the gas flow contains nine main species. The inflow radius is about 0.04 m. Non-uniform inflow boundary conditions are used at the nozzle exit based on the gas flow simulation inside the nozzle, and the mean values of the inflow gas parameters are listed in Table 3. The mass fractions of the gas species are shown in Table 4. The liquid phase mainly contains liquid droplets of MMH and NTO. At the exit of the nozzle the total mass fraction of the liquid droplet is about 2.66%. Because of the relatively low mass fractions of unburnt liquid droplets, only gas-to-particle one-way coupling is conducted in the present study. Other inlet conditions of the liquid phase are listed in Table 5.

In the calculation, a two-dimensional computation domain is set with a scale of 0.4 m × 0.3 m, and the nozzle exit center is coincident with the origin of coordinate, while, the *x*-axis is the axis of symmetry. To estimate the cell size and time step interval, a pure DSMC calculation is run firstly for the gas flow

**Table 3** Mean values of inlet gas parameters.

| Pressure (Pa) | Temperature (K) | Density (kg·m$^{-3}$) | Mach number |
|---|---|---|---|
| 1100 | 1000 | $2.79 \times 10^{-3}$ | 3.35 |

**Table 4** Mass fractions of gas species.

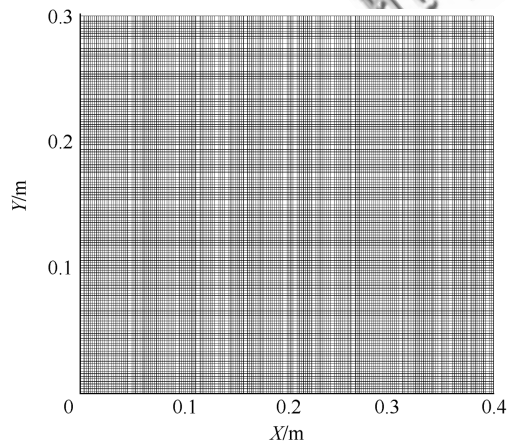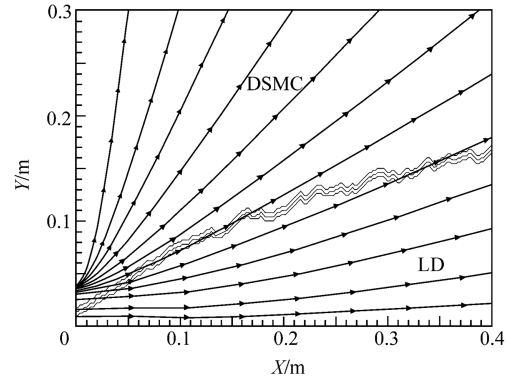| Index | Species | Mass fraction |
|---|---|---|
| 1 | $N_2$ | 0.2724 |
| 2 | $CO_2$ | 0.0618 |
| 3 | $H_2O$ | 0.1426 |
| 4 | CO | 0.0759 |
| 5 | $H_2$ | 0.0214 |
| 6 | $NO_2$ | 0.0797 |
| 7 | NO | 0.1788 |
| 8 | $O_2$ | 0.0953 |
| 9 | $CH_4$ | 0.0721 |

**Table 5**    Average parameters of inlet liquid particles.

| Species | Velocity magnitude (m·s$^{-1}$) | Temperature (K) | Mass flow (kg·s$^{-1}$) | Diameter (m) |
|---|---|---|---|---|
| MMH | 900 | 227 | $4.0 \times 10^{-5}$ | $3.0 \times 10^{-5}$ |
| NTO | 800 | 190 | $3.6 \times 10^{-5}$ | $2.83 \times 10^{-5}$ |

without liquid droplets. Results show that the mean free path of the gas flow varies from $10^{-5}$ m to 0.2 m, and the mean collision time is within $10^{-8}$ s to $10^{-4}$ s. Although the DSMC simulation requires a cell size and time step compared to the mean free path and mean collision time, respectively, the regions with high gas densities are expected to be simulated by the LD method in the hybrid calculation, and relatively large cell size and time step can be used. By taking into consideration of both the flow properties and the computation efficiency, a uniform cell size of 0.002 m and a time step of $10^{-7}$ s are used in this case. Fig. 6 illustrates the computation domain and grid. Thirty thousand time steps of computation are run. After about 20000 steps, it is observed that the total number of particles in the domain has changed very little and the flow is regarded to reach a steady state. The last 10000 time steps are sampled to obtain the results. Before sampling procedure, the continuum breakdown parameter is calculated every 100 steps to assigned computation type for each cell. As the cell volumes change a lot in an axial simulation, a gas particle weight is also assigned to ensure smooth particle distributions in each cell. Gas particles which cross cells with different weights should be determined to clone or remove.[2] Finally, at the steady state, about 0.6 million gas particles and 5000 liquid particles are present in the flow field. This simulation cost 40 h CPU time on eight processors.

Based on the primary DSMC results, even in the near-continuum regions, the condensed particle Knudsen number is higher than 0.1 due to the small sizes of the liquid droplets. Hence, Eqs. (19) and (24) are used to estimate the drag coefficient and Nusselt number, respectively, in the condensed particle motion and temperature relaxation treatments.

The streamlines of the hybrid solution is shown in Fig. 7, along with boundaries of the LD and DSMC regions at the end of the sampling period. The LD region is in the core region of the plume field and the DSMC domain locates around the LD one, which indicates that the flow in the core of the plume



**Fig. 7**    Streamlines of gas flow and boundaries between LD and DSMC regions.

field belongs to continuum flow with high density. The light solid lines in the figure denote the cells within the boundary buffer between LD and DSMC regions. In contamination analysis, the amount of the contaminants might be the most interesting parameter. The mass fractions and volume fractions of the two liquid-phase species are illustrated in Figs. 8–11. The mass fraction $\phi$ and volume fraction $\alpha$ are defined as[16]

$$\phi_k = \frac{\delta m_k}{\delta m}, \quad \alpha_k = \frac{\delta V_k}{\delta V} \tag{33}$$

where $m_k$ and $V_k$ are the mass and volume of the liquid phase, while $m$ and $V$ denote the mass and volume of mixtures, respectively.

The distributions of the volume fractions illustrate that the liquid droplets are firstly concentrated in the vicinity of the nozzle exit, then, they mainly scatter in the core region of the plume due to the effect of motion. In the region near the nozzle exit, the large gradients of the macro-parameters result in a limited LD domain; therefore, the liquid particles appear both in the DSMC and LD domains. As the plume expands, the gas density reduces significantly, and the mass fractions of the liquid-phase increase correspondingly. However, Eqs. (9), (16), (20) and (26) show that the momentum increase in gas phase is proportional to the quantity $\sum d_{p,j}^2 / V_{cell}$, if only the drag force is included. Hence, due to the low volume fractions, the one-way particle-to-gas evaluation is still reasonable. From the distributions of the mass fractions, it is observed that the maximum value for a given $X$ value tends to be slightly off-axis. The main reason is that at the nozzle exit, peak values of the liquid mass flow appear off the $X$-axis. Because of the very low amount of the liquid droplets, the statistical scatter effects are easily observed in the figures. However, these scatters are not the same as the ones related to the random motion of the microscopic particles. This statistical scatter might reflect the non-uniform distributions of the macroscopic droplets in space. It might be mentioned that the accuracy of this case is highly dependent on the accuracy of the inlet condition
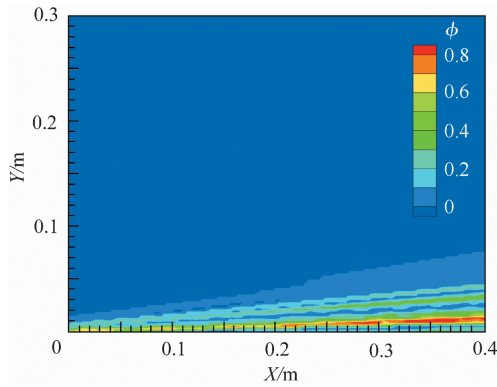


**Fig. 6**    Computational domain and grid of hybrid simulation.

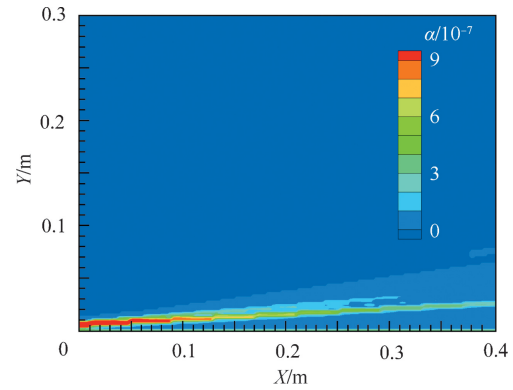**Fig. 8** Contour of liquid MMH mass fraction.



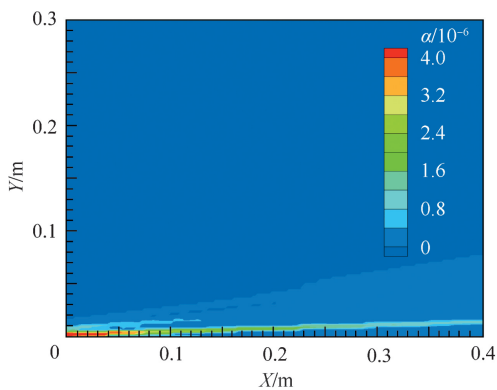**Fig. 11** Contour of liquid NTO volume fraction.



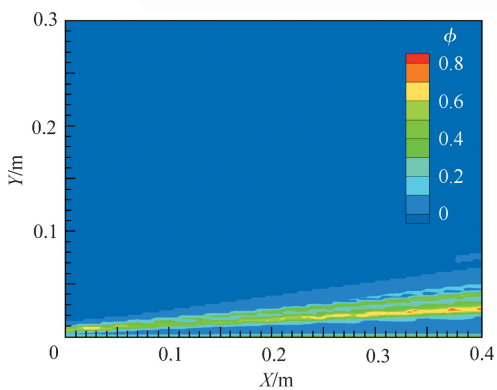**Fig. 9** Contour of liquid MMH volume fraction.



**Fig. 10** Contour of liquid NTO mass fraction.

of the liquid droplets. In the future, we will conduct experimental tests to investigate the flow structure and droplet distributions when the experimental devices and other conditions are available.

This simple case demonstrates that the hybrid LD–DSMC algorithm is promising for two-phase flow simulations. In future works, tests on the accuracy and efficiency of this hybrid simulation should be considered.

## 5. Conclusions

(1) A brief introduction to the LD method and the hybrid LD–DSMC algorithm is stated. The LD method is proposed by Burt and Boyd, and used for simulations of near-continuum gas flows. The LD method is attractive because it can reduce the numerical diffusion error and statistic scatter of the published equilibrium particle method, and can be easily coupled with the DSMC method in a hybrid algorithm.

(2) Based on the original one, the LD method has been extended for near-continuum two-phase flows in this paper. The motion and temperature relaxations of the condensed phase are directly obtained from the drag effect and heat transfer, and the changes of condensed-phase velocity and temperature are calculated, respectively, through motion equations and temperature change equations. The effects of the condensed phase on the gas phase are modeled as momentum and energy source, which should be considered during velocity and temperature updating of the LD gas particles.

(3) Results from a series of unsteady two-phase flow simulations using the modified LD method are compared with their corresponding theoretical solutions. Overall excellent agreement is achieved, which indicates the validity of the one-way implementation of particle motion and temperature relaxations. However, further tests on mutual particle–gas interactions should be considered in the future.

(4) The modified LD method is embedded into a DSMC code for two-phase flow simulations. A gas–liquid flow discharged from a nozzle into vacuum environment can be simulated, which indicates the prospects of the hybrid LD–DSMC algorithm. Due to the relatively low mass and volume fractions of the liquid phase, only gas-to-particle one-way coupling is presented. More test works for the hybrid algorithm will be carried out in the future, including numerical verifications and experimental tests.

(5) Although the particle-to-gas coupling procedures are proposed in this paper, no reliable works have been conducted to validate the scheme. The main reason is that, in a flow with dilute condensed-phase, the

particle-to-gas effect is too weak to be captured among the statistical noise of the particle-based method. However, it should be mentioned that a lack of these procedures may contribute significantly to errors, when the mass fraction of the condensed phase becomes large enough. Again, further works will focus on the evaluation of the particle-to-gas effect.

## Acknowledgement

## References

1. Shen Q. *Rarefied gas dynamics*. Beijing: National Defense Industry Press; 2003 [Chinese].
2. Bird GA. *Molecular gas dynamics and the direct simulation of gas flow*. 2nd ed. Oxford: Clarendon Press; 1994.
3. Laux M. *Local time stepping with automatic adaptation for the DSMC method*; 1998. Report No.: AIAA-1998-2670.
4. Boyd ID, Penko PF, Meissner DL, DeWiit KJ. Experimental and numerical investigations of low-density nozzle and plumes of nitrogen. *AIAA J* 1992;**30**(10):2453–61.
5. Hash DB, Hassan HA. *A decoupled DSMC/Navier–Stokes analysis of a transitional flow experiment*; 1996. Report No.: AIAA-1996-353.
6. Bird GA. Near continuum impact of an under-expanded jet. In: *Proceedings of AIAA computational fluid dynamics*; 1973. p. 103.
7. Pullin DI. Direct simulation methods for compressible ideal gas flow. *J Comput Phys* 1980;**34**(2):231–44.
8. Macrossan MN, Metchnik MV, Pinto PA. Hypersonic flow over a wedge with a particle flux method. In: *24th international symposium on rarefied gas, dynamics*; 2004. p. 650–6.
9. Burt JM, Boyd ID. A low diffusion particle method for simulating compressible inviscid flows. *J Comput Phys* 2008;**227**(9):4653–70.
10. Burt JM, Boyd ID. A hybrid particle approach for continuum and rarefied flow simulation. *J Comput Phys* 2009;**228**(2):460–75.
11. Burt JM, Boyd ID. Extension of a multiscale particle scheme to near-equilibrium viscous flows. *AIAA J* 2009;**47**(6):1507–17.
12. Burt JM, Boyd ID. *Rotational and vibrational nonequilibrium in a low diffusion particle method for continuum flow simulation*; 2009. Report No.: AIAA-2009-3743.
13. Burt JM, Boyd ID. *Application of a multiscale particle scheme to high altitude rocket exhaust flows*; 2009. Report No.: AIAA-2009-1567.
14. Burt JM, Boyd ID. *A hybrid particle scheme for simulating multiscale gas flows with internal energy nonequilibrium*; 2010. Report No.: AIAA-2010-820.
15. Jun E, Brut JM, Boyd ID. *All-particle multiscale computation of hypersonic rarefied*; 2010. Report No.: AIAA-2010-822.
16. Gimelshein SF, Alexeenko AA, Wadsworth DC, Gimelshein NE. *The influence of particulates on thruster plume/shock layer interaction at high altitudes*; 2005. Report No.: AIAA-2005-766.
17. Liu D. *Fluid dynamics of two-phase systems*. Beijing: High Education Press; 1993 [Chinese].
18. Guo L. *Two-phase and multi-phase fluid dynamics*. Xi'an: Xi'an Jiaotong University Press; 2002 Chinese.
19. Poling BE, Prausnitz JM, O'Connell JP. *The properties of gases and liquids*. 5th ed. New York: Mc Graw Hill Press; 2001.
20. He X, He B, Cai G. Simulation of rocket plume and lunar dust using the direct simulation Monte Carlo method. *Acta Astronaut* 2012;**70**:100–11.
21. Gallis MA, Torczynski JR, Rader DJ. An approach for simulating the transport of spherical particles in a rarefied gas flow via the direct simulation Monte Carlo method. *Phys Fluids* 2001;**13**(11):3482–92.
22. Burt JM, Boyd ID. *Development of a two-way coupled model for two phase rarefied flows*; 2004. Report No.: AIAA-2004-1351.
23. Bird GA. Breakdown of translational and rotational equilibrium gaseous expansions. *AIAA J* 1970;**8**(11):1998–2003.
24. Boyd ID, Chen G, Chandler G. Predicting failure of the continuum fluid equations in transitional hypersonic flows. *Phys Fluids* 1995;**7**(1):210–9.
25. Wang W, Boyd ID. *Continuum breakdown in hypersonic viscous flows*; 2005. Report No.: AIAA-2005-651.
26. Wang W, Sun Q, Boyd ID. *Towards development of a hybrid DSMC–CFD method for simulating hypersonic interacting flows*; 2002. Report No.: AIAA-2002-3099.
27. Bauman SD. *A spray model for an adaptive mesh refinement code* dissertation. Madison (MI): University of Wisconsin – Madison; 2001.
28. Tang Z, Hou F, Cai G. A model for simulating the operating process of combustion chamber of bipropellant attitude-control engine. *J Propul Technol* 2012;**33**(2):193–7 [Chinese].

**Su Wei** is a Ph.D. student at Beihang University. Her main research interest is computational rarefied gas dynamics.

**He Xiaoying** is a Ph.D. student at Beihang University. Her main research interest is DSMC simulation for multiple phase rarefied gas flows.

**Cai Guobiao** is a professor at Beihang University. His main research interests are vacuum plume and its effects, hybrid rocket engine technology, and reusable rocket engine technology.